

TABLE 2. |ERROR|  $\times 10^5$  AT VARIOUS  $x$ . ONE EXTRAPOLATION

All calculations start with  $\Delta x = 0.2$ .  
Error is recorded at  $t = 0.512$  for  $\rho = 0.8$ .  
Error is recorded at  $t = 0.5$  for  $\rho = 1.25$ .

Method	Scheme	$\rho$	$x = 0.2$	$x = 0.6$	$x = 0.8$	Com- puting time
CN	A	0.80	5.3	3.2	1.7	0.50
CN	B	0.80	6.1	3.9	2.0	0.54
CN	A	1.25	17.1	10.4	5.2	0.39
CN	B	1.25	14.2	9.1	4.6	0.42
SRL	B	0.80	382.8	182.2	75.4	0.34
SRL	B	1.25	525.4	185.6	43.4	0.30
SA	B	0.80	74.4	64.0	42.5	0.42
SA	B	1.25	190.9	160.6	92.5	0.32
LRL	B	0.80	122.6	34.4	3.4	0.39
LA	B	0.80	66.1	37.6	6.7	0.50

sively smaller spacings.

As an introduction to the extrapolation results, we present in Table 1 data on the standard case (no extrapolation). These correspond to extensions of Tables 1 and 2 of Liu. Of primary interest here is that these calculations completely confirm Wilke's comments on the validity of the Crank-Nicholson algorithm and also suggest that the errors given by Liu for the Saul'yev method were inordinately large. The results shown with an asterisk were an independent set of calculations. It is difficult to specify that any of the methods, CN, S, or L, are significantly better (more accurate or faster) than the others.

The superiority of the extrapolated results is apparent from Tables 1 to 3, with Tables 2 and 3 presenting extrapolated data. Using the Crank-Nicholson results as an illustration, we see that with one extrapolation we can achieve the accuracy of the nonextrapolation case but with one-quarter of the computing time. Two extrapolations show that for roughly the same computing time results can be obtained which are a thousandfold more accurate. Obviously, either in terms of higher accuracy or decreased computer time, the extrapolation algorithm is significantly better than the nonextrapolated procedure.

TABLE 3. |ERROR|  $\times 10^5$  AT VARIOUS  $x$ . TWO EXTRAPOLATIONS

All calculations start with  $\Delta x = 0.2$ .  
Error is recorded at  $t = 0.512$  for  $\rho = 0.8$ .  
Error is recorded at  $t = 0.5$  for  $\rho = 1.25$ .

Method	Scheme	$\rho$	$x = 0.2$	$x = 0.6$	$x = 0.8$	Com- puting time
CN	A	0.80	0.0146	0.0068	0.0031	2.36
CN	B	0.80	0.008	0.0034	0.0014	2.48
CN	A	1.25	0.075	0.042	0.0107	1.57
CN	B	1.25	0.009	0.0003	0.0177	1.66
SRL	B	0.80	30.4	13.3	3.04	1.00
SA	B	0.80	2.88	3.97	6.19	1.39
LRL	B	0.80	17.2	9.2	6.4	1.21
LA	B	0.80	0.2	1.4	1.6	1.89

Furthermore, these results show that of the three basic algorithms the Crank-Nicholson method is best when used in an extrapolation format.

Once again we emphasize that these results are given to show briefly the power of extrapolating known algorithms. A forthcoming publication will deal more specifically with aspects of the types of P.D.E.'s, with the form of truncation errors, with stability and round-off errors, with different modes of implementation of extrapolation, and with nonlinear problems.

#### ACKNOWLEDGMENT

This work was performed with the assistance of a grant from the National Science Foundation, GP-506. Computations were carried out using the facilities of the Princeton University Computer Center, supported in part by NSF Grants GJ-34 and GU-3157.

#### LITERATURE CITED

1. Hlavacek, V., *Ind. Eng. Chem.*, **62** (7), 8 (1970).
2. Liu, S., *AIChE J.*, **15**, 334 (1969).
3. Ralston, A., and H. S. Wilf, "Mathematical Methods for Digital Computers," Vol. II, p. 133, Wiley, New York (1967).
4. Wilkes, J. O., *AIChE J.*, **16**, 501 (1970).
5. Wyman, C. E., private communication (Aug. 1970).

## A Test of the Inertial Theory for Plate Withdrawal

ANTHONY J. SOROKA and JOHN A. TALLMADGE

Drexel University, Philadelphia, Pennsylvania

Consider the viscous entrainment of thin films of wetting liquids on flat supports by continuous steady state withdrawal. One of many bath arrangements for such a free coating process is shown in Figure 1. In particular, consider the prediction of film thickness  $h_0$  (in the constant thickness region above the meniscus) as a function of constant withdrawal speed  $U_w$ , together with the influence of fluid properties ( $\mu$ ,  $\sigma$ ,  $\rho$ ). This problem has several applications in coating, cleaning, and lubrication processes (6). The mass flow rate entrained  $w$  by a plate of width  $b$  is related to the film thickness  $h_0$  by the Nusselt type of expression

$$w = \rho U_w b h_0 \left[ 1 - \frac{h_0^2 \rho g}{3\mu U_w} \right] \quad (1)$$

One new method of discussing this problem is to consider simultaneously the effect of four forces, namely that of inertia, surface tension, viscosity, and gravitational field. The nondimensional groups describing these four forces have been given (7) as fluid property number  $Fp \equiv \mu(g/\rho\sigma^3)^{1/4}$ , nondimensional speed  $Ca \equiv U_w(\mu/\sigma)$ , and thickness  $D \equiv h_0(\rho g/\sigma)^{1/2}$ . Thus the desired expression showing how thickness increases with speed may be described as

$$h_0 \left( \frac{\rho g}{\sigma} \right)^{1/2} = \phi_1 \left[ \frac{U_w \mu}{\sigma}, \mu \left( \frac{g}{\rho \sigma^3} \right)^{1/4} \right] \quad (2)$$

or

$$D = \phi_1(Ca, Fp) \quad (2a)$$

One equivalent form of Equation (2a) involves Reynolds

A. J. Soroka is with the duPont Company, Wilmington, Delaware.

number  $N_{Re}$  in place of  $Fp$ ; that is,  $D = \phi_2(Ca, N_{Re})$ . Although the function involving  $N_{Re}$  is convenient for understanding, it is inconvenient here because withdrawal  $N_{Re}$  is a dependent variable (unlike downward wetted wall flow, where  $N_{Re}$  is an independent variable). This difficulty with  $N_{Re}$  led to the choice of the independent variable  $Fp$  (7). From the viewpoint of experimental variables,  $Fp$  is a nondimensional viscosity. The withdrawal Reynolds number which is consistent with wave formation and wetted wall flow has been developed, defined, and expressed in terms of  $Fp$  as follows (7):

$$N_{Re} = \frac{h_0^3 \rho^2 g}{3\mu^2} \equiv \frac{D^3}{3Fp^2} \quad (3)$$

One new method of predicting film thickness theoretically is to integrate a simplified form of the Navier-Stokes equation for thin films, given by (4, 5)

$$\rho U_w \frac{\partial u}{\partial x} = \sigma \frac{d^3 h}{dx^3} + \mu \frac{\partial^2 u}{\partial y^2} - \rho g \quad (4)$$

Equation (4) is a four-force equation which has been solved, but for editorial reasons the development is not presented here. The approximate theoretical solution to Equation (4) is (4, 5)

$$Ca = 1.09D^{3/2} + D^2 + 0.50\beta D^2 \quad (5)$$

Here

$$\beta = \exp \left[ -\frac{5.13Fp^2}{Ca^{4/3}D} \right] = \exp \left[ -\frac{1.71D^2}{Ca^{4/3}N_{Re}} \right] \quad (6)$$

Equation (5) is called the *inertial theory of plate withdrawal*. The purpose of this note is to test Equation (5) with precise experimental data. Equation (5) is the quantitative, analytical description of the function implied by Equation (2a), namely the influence of  $Fp$  and  $Ca$  on entrainment.

## TEST CONDITIONS REQUIRED

Data was available at  $Ca$  from about  $10^{-4}$  to about 5. To avoid duplication, results of tests of earlier theories (9) are considered first, starting at low  $Ca$ . The two-force, Landau-Levich solution of Equation (4) for negligible inertia and gravity led to the viscosurface theory given by  $Ca = 1.09D^{3/2}$ . Thus thickness was predicted to be a function of speed to the two-thirds power. Data confirmed this theory at low speeds (low  $Ca$  and low  $D$ ), but substantial deviations were noted above  $Ca$  of  $10^{-2}$ .

The two-force, Deryagin solution of Equation (4) for negligible inertia and surface tension led to the viscogravity theory given by  $Ca = D^2$ . Thus thickness was predicted to be a function of speed to the one-half power. The same speed effect is given by another viscogravity theory which differs from  $Ca = D^2$  only by a constant (1). Tests of both viscogravity theories at low speeds indicated substantial deviations in predicting both magnitude and influence of speed (1, 9). Thus the viscogravity theories are rejected as valid, wide speed theories.

The three-force solution of Equation (4) for negligible inertia led to (9)

$$Ca = 1.09D^{3/2} + D^2 \quad (7)$$

Because Equation (7) agrees within 15 to 20% for all  $Ca$  data available (1, 9), it is the best theory previously available. The available data (1, 9) also confirm that the capillary number is the suitable parameter for drawing together the data of several fluids at low speeds, although some scatter occurs at higher capillary numbers.

Now compare Equation (5) with Equation (7). At low  $N_{Re}$  resulting from low  $Ca$  (7), Equation (6) shows

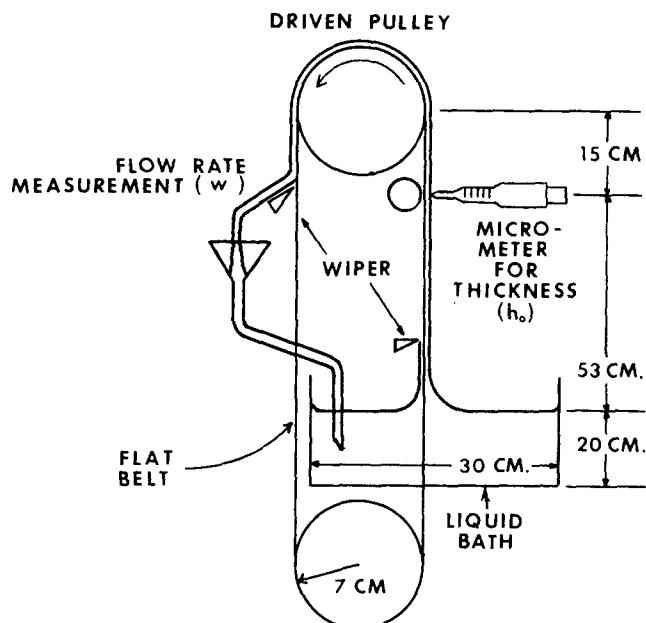


Fig. 1. Withdrawal apparatus (Van Rossum bath).

that  $\beta \rightarrow 0$ . Thus the four-force theory reduces to Equation (7) at low  $Ca$ . We conclude, therefore, that a test of Equation (5) requires comparison with Equation (7) at higher  $Ca$  than the  $Ca$  values studied earlier. Experimentally, higher  $Ca$  implies higher speeds and/or high viscosities, since liquid-gas surface tensions are constant within a factor of 2 for most liquids at room temperature.

The study at higher speeds and higher  $Ca$  is also an important problem industrially, because it is often desirable to operate at high speeds for reasons of productivity and economy. Such high-speed trends have occurred in many coating applications, including those related to photographic films, textile fibers, and galvanizing of steel.

## EXPERIMENTAL CONDITIONS

Experimental aspects are briefly summarized here. Further details are available in thesis form (4). The three Newtonian oils selected had high viscosities of 0.533, 2.46, and 19.3 poise, respectively (fluids P, M, and B) in order to obtain higher  $Ca$  values. The values of surface tension and density did not vary appreciably; they were 29.7, 31.0, and 32.6 dynes/cm. and 0.869, 0.875, and 0.885 g./cc. for P, M, and B, respectively.

The temperature was held at  $72.0 \pm 0.5^\circ\text{F}$ . for measurements of both fluid properties and withdrawal entrainment.

A schematic diagram of the experimental apparatus is shown in Figure 1. The endless, stainless steel belt was made by carefully welding together the ends of a long sheet. The belt was 6.2 cm. wide and was positioned between two pulleys of which the upper was driven by an adjustable speed drive system. The method and apparatus was based on that described by Gutfinger and Tallmadge (2, 3). The dimensions of the pulleys, bearings, and several other parts were identical to those of Gutfinger (2). Two of the modifications to Gutfinger's design made for this work included an improved liquid bath (revised location and larger size), and an improved speed control and measurement.

In previous work and in preliminary work here, the pulley was immersed in the liquid bath (2, 3); this is called the *Gutfinger bath location* for low speeds. To

eliminate the flow effects noted previously with the Gutfinger bath (2, 3), the bath location was changed so that the belt passed through the bottom of the bath. The new location, shown in Figure 1, was patterned after that of Van Rossum (8). Preliminary studies showed the change was effective. Specifically, the amount of air entrainment was visually observed to be reduced by the change. Furthermore, surface waves were reduced; wave onset speeds with the Van Rossum bath were about 30% larger than with the Gutfinger bath apparatus (4). The elimination of flow effects due to the lower pulley probably accounts for the increase in wave point speeds. As described elsewhere (7), the speed for the onset of wavy flow has been correlated as occurring at a withdrawal  $N_{Re}$  of about 1.

The large liquid bath was made of 1 cm. thick clear Plexiglas, 30 cm. long, 23 cm. wide, and 23 cm. high. The experimental data were taken for a liquid depth of  $20 \pm 1$  cm. and a belt-to-bath wall distance of 18 cm.

The upper pulley was driven by a precision speed controlled motor and a solid state, speed reduction unit. A new system of timing belts and pulleys were used to connect the drive mechanism with the upper pulley and prevent slipping. A 1:6.86 speed ratio set was used to provide withdrawal speeds up to 105 cm./sec.

Pulley speeds were measured with a tachometer for each run in order to obtain more precise run values than those obtained previously by using calibration curves. As before, the speed of the  $\frac{3}{4}$ -hp. motor was set by a 1,000 division potentiometer.

## EXPERIMENTAL MEASUREMENTS

To improve precision, two other modifications to Gutfinger's technique were made. They included an improved film thickness measurement (modified micrometer tip and use of lights), and an improved flow rate measurement (wiper design).

The film thickness  $h_0$  was measured directly at the horizontal center of the belt by means of a micrometer apparatus and at a height of about 53 cm. above the liquid surface. Preliminary investigations were made to determine the effects of both geometry on film thickness. Specifically, the errors resulting from use of a finite bath (to approximate an infinite quiescent bath) were found to be negligible for the bath geometry used in this work (5).

The tip of the micrometer barrel (2) was changed by machining to a fine point (angle  $\sim 2$  deg.) to minimize the amount of liquid adhering to it after each contact with the film. To improve the visual measurement, lights were

positioned in the same horizontal plane as the micrometer and at an angle of about 30 deg. to the belt. The resultant film reflection helped determine when the micrometer liquid contact point had been obtained. Six to ten thickness measurements were made per run, depending on the reproducibility of each succeeding measurement. Variations of about  $\pm 0.0002$  to  $\pm 0.001$  cm. in the reading to-reading micrometer measurements were observed for films from 0.043 to 0.966 cm. thick. The median deviation for all runs was 0.1%, which is an improvement compared with Gutfinger's (2) median value of 0.8%. The deviation for 90% of the runs was 0.2% or less, whereas Gutfinger's (2) value was 1.6%.

Mass flow rate measurements ( $w$ ) were taken for an independent test of the theory. They were obtained by collecting all the liquid wiped from the front side of the belt over a given period of time. Three measurements were taken for each run, and large samples were taken to minimize weighing and time errors. Two new wipers consisted of  $3\frac{1}{2}$  in. long strips of neoprene rubber mounted on a spring loaded holder. The blades were tapered and held tightly against the belt to insure complete wiping of the liquid from the belt. Variations of about  $\pm 0.05$  to  $\pm 1.0$  g. in the reading-to-reading mass measurements resulted in relative deviations of 0.5% (median) to 0.7% (80% level) in mass flow rate. In Gutfinger's work, the relative deviations were 1.1 (median) and 1.4% (80% level).

## FILM THICKNESS RESULTS

To permit illustration of data in measured, dimensional form, the theories given above as  $D = \phi(Ca, F_p)$  are expressed in terms of  $h_0 = \phi_1(U_w, \mu)$ . In the following discussion, new withdrawal data obtained with the Figure 1 apparatus are compared with the inertial theory of Equation (5) and with Equation (7). Equation (7) has been called the gravity corrected theory (GCT); it is a special case of Equation (5) for  $\beta = 0$ .

Film thickness data for the 19-poise fluid, as shown in Figure 2, indicate better agreement with the inertial theory. The average deviation of the inertial theory from data is only about 1.5%. The capillary numbers of 3 to 44 shown in Figure 2 indicate that verification of the inertial theory has been extended up to a  $Ca$  of 44.

At speeds above 50 cm./sec., film thickness deviate considerably from the gravity corrected theory; the deviation was about 10% at 74 cm./sec. For this fluid, deviations appear at  $Ca$  above 30. The fact that the inertial

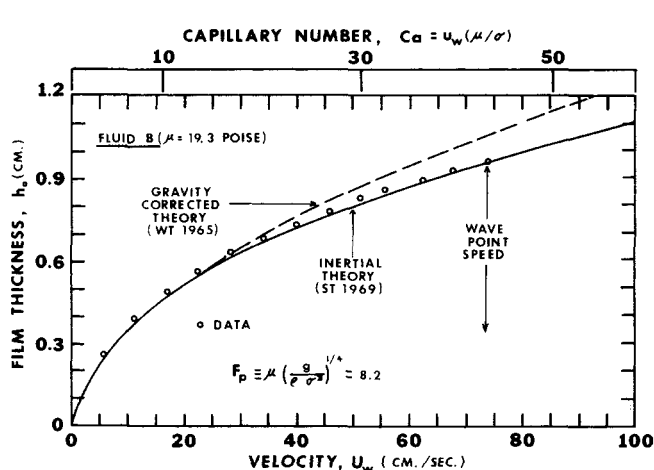


Fig. 2. Thickness data for the 19-poise fluid. — Inertial theory, Equation (5). - - - Previous theory, Equation (7).

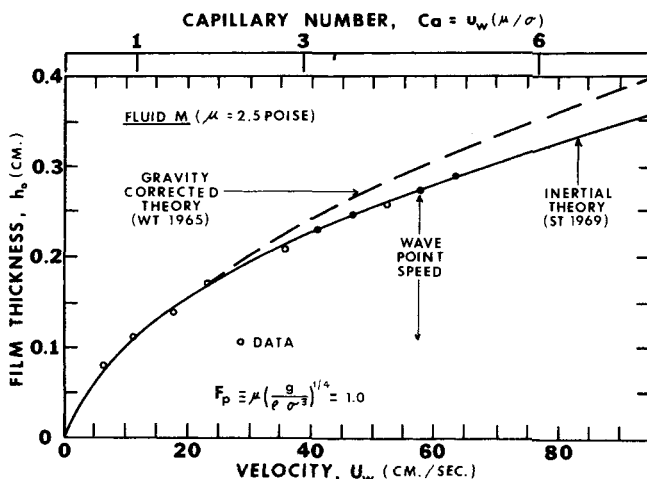


Fig. 3. Thickness data for the 2.5-poise fluid. — Inertial theory, Equation (5). - - - Previous theory, Equation (7).

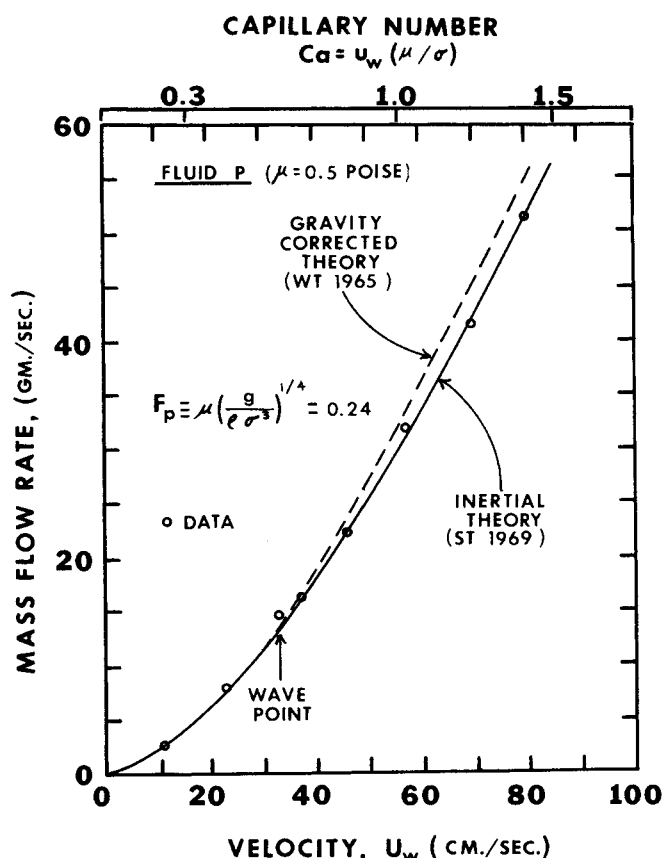


Fig. 4. Mass flow rate data for the 0.5-poise fluid. — Inertial theory, Equation (5). - - - Previous theory, Equation (7).

theory fits the data better than the GCT at high  $Ca$  shows the importance of inertial forces (and  $N_{Re}$ ) at high speeds. Because film thickness data are not reliable above the wave point speed, no thickness data were taken above 74 cm./sec. for this 19-poise fluid. The wave point speeds are discussed elsewhere (7).

Similar results were obtained for the 2.5-poise fluid, as shown in Figure 3. Deviations from the GCT appeared above 40 cm./sec. (or  $Ca$  of 3 for this fluid) and were about 7% at 57 to 63 cm./sec. The inertial theory fits the data over a wide speed range with an average deviation of about 1%. Thus the significance of the inertial forces at high speeds is confirmed for a 2.5-poise fluid. Figures 2 and 3 also confirm the Equation (5) effect of  $F_p$ , a parameter which does not appear in Equation (7).

Only a few thickness data were taken with the 0.5-poise fluid because of wave limitations. Owing to low viscosity and a lower wave speed of 37 cm./sec., the maximum attainable  $Ca$  for film thickness was 0.6. On a thickness-speed plot, the resulting data generally agreed with both theories, as expected.

## FLOW RATE RESULTS

Theoretical predictions of mass flow rate were obtained from theoretical  $h_0$  values by use of Equation (1). Flow rate measurements ( $w$ ) for the 0.5-poise fluid, given in Figure 4, show that the inertial theory fits the data closely (average deviation less than 1%) and that the gravity corrected theory deviates from the data (10% at a speed of 70 cm./sec.). Thus flow rate data confirm the superiority of the inertial theory to the previous theory. Similar agreement in flow rate was obtained by using the 2.5-poise fluid.

Figure 4 also shows that meaningful mass flow rates

can be measured above the wave point speed, as well as below. No flow rate measurements were taken for the 19-poise fluid owing to equipment problems. Entrainment was so large that, as fluid was wiped from the back surface of the belt (Figure 1), surface tension forces caused some liquid to flow away from the measurement side of the belt. Consistently lower mass flow rates resulted. Film thickness ( $h_0$ ) measurements were not affected for this fluid, since they were taken in the center of the belt.

## CONCLUSIONS

1. The precision of withdrawal data was improved in comparison to earlier work (2), due partly to larger films and partly to improvements in the experimental technique.
2. The experimental range of  $Ca$  was extended to  $Ca$  of 44.
3. The inertial theory was verified by data of this work at higher  $Ca$  and by previous work at lower  $Ca$ . The theory fit all the data of this work with a median deviation of less than 1.5%. The verified range is about 6 cycles in  $Ca$  ( $6 \times 10^{-5}$  to  $4 \times 10^{+1}$ ), and the theory is probably a good approximation at  $Ca$  above and below this range.
4. The theory is useful for film thickness predictions up to the wave point speed. Flow rate predictions are valid both below and above the wave point speed.

## ACKNOWLEDGMENT

The authors are grateful for the National Science Foundation Grant GK-1206 by which this work was supported.

## NOTATION

- $b$  = belt width, cm.  
 $Ca$  = capillary number,  $\mu U_w \sigma$   
 $D$  = nondimensional thickness,  $h_0(\rho g / \sigma)^{1/2}$   
 $F_p$  = fluid property number,  $\mu(g / \rho \sigma^3)^{1/4}$   
 $g$  = gravitational acceleration, cm./sec.<sup>2</sup>  
 $h$  = film thickness in the meniscus, cm.  
 $h_0$  = film thickness, constant thickness region, cm.  
 $N_{Re}$  = withdrawal Reynolds number,  $h_0^3 \rho^2 g / 3 \mu^2$ , Equation (3)  
 $u$  = local velocity parallel to the belt, cm./sec.  
 $U_w$  = velocity of the belt, cm./sec.  
 $w$  = mass flow rate, g./sec.  
 $x$  = coordinate parallel to the belt, cm.  
 $y$  = coordinate perpendicular to the belt, cm.  
 $\beta$  = nondimensional parameter, Equation (6)  
 $\mu$  = liquid viscosity, poise  
 $\rho$  = liquid density, g./cc.  
 $\sigma$  = surface tension of the liquid-air interface, dyne/cm.

## LITERATURE CITED

1. Groenveld, P., *Chem. Eng. Sci.*, **25**, 33 (1970).
2. Gutfinger, Chaim, Ph.D. dissertation, Yale Univ., New Haven, Conn. (Aug. 1964).
3. —, and J. A. Tallmadge, *AIChE J.*, **11**, 403 (1965).
4. Soroka, A. J., Ph.D. dissertation, Drexel Inst. Technol., Philadelphia, Pa. (June, 1969).
5. —, and J. A. Tallmadge, paper presented at Am. Inst. Chem. Engrs. Annual Meeting, Washington, D. C. (Nov., 1969).
6. Tallmadge, J. A., and Chaim Gutfinger, *Ind. Eng. Chem.*, **59**, No. 11, 18 (1967). Corrections in **60**, No. 2, 74 (1968).
7. Tallmadge, J. A., and A. J. Soroka, *Chem. Eng. Sci.*, **24**, 377 (1969).
8. Van Rossum, J., *J. Appl. Sci. Res.*, **A7**, 121 (1958).
9. White, D. A., and J. A. Tallmadge, *Chem. Eng. Sci.*, **20**, 33 (1965).